

# Neuropathologic findings in a young woman 4 years following declaration of brain death: case analysis and literature review

Rebecca D. Folkerth , MD\*<sup>1</sup>, John F. Crary, MD, PhD<sup>1</sup>, D. Alan Shewmon, MD<sup>1</sup>

<sup>1</sup>From the New York University Grossman School of Medicine, New York City Office of Chief Medical Examiner, New York, New York, USA (RDF); Departments of Pathology, Neuroscience and Artificial Intelligence & Human Health, Ronald M. Loeb Center for Alzheimer's Disease, Neuropathology Brain Bank & Research Core, Friedman Brain Institute, Icahn School of Medicine at Mount Sinai, New York, New York, USA (JFC); and Departments of Pediatrics and Neurology, David Geffen School of Medicine at UCLA, Los Angeles, California, USA (DAS)

\*New York City Office of Chief Medical Examiner and New York University Grossman School of Medicine, 520 First Avenue, New York, NY 10016, USA; E-mail: rfolkerth@gmail.com; rfolkerth@ocme.nyc.gov; rebecca.folkerth@nyulangone.edu

## ABSTRACT

Brain death (death by neurologic criteria) is declared in 2% of all in-hospital deaths in the United States. Published neuropathology studies of individuals maintained on cardiorespiratory support are generally decades old, and notably include only 3 cases with long intervals between brain and “somatic” death (68 days, 101 days, 20 years). Here, we share our observations in a young woman supported for nearly 4½ years following declaration of brain death after oropharyngeal surgery. While limited by tissue availability and condition, we found evidence of at least partial perfusion of the superficial cerebral and cerebellar cortices by external carotid and vertebral arteries (via meningeal and posterior pharyngeal branches), characterized by focal cellular reaction and organization. Dural venous sinuses had thrombosis and recanalization, as well as iron deposition. In nonperfused brain areas, tissue “mummification,” akin to that seen in certain postmortem conditions, including macerated stillbirths and saponification (adipocere formation), was identified, and are reviewed herein. Unfortunately, correlation with years-earlier clinical and radiographic observations was not possible. Nevertheless, we feel that our careful neuropathologic inspection of this case expands the understanding of the spectrum of human brain tissue alterations possible in a very rarely seen set of conditions.

**KEYWORDS:** Adipocere, Autolysis, Brain death, Mummification, Postmortem, Respirator brain

## INTRODUCTION

The annual incidence of declaration of brain death, or death by neurologic criteria (1, 2), has been estimated at approximately 39 per 100 000 hospital discharges, representing approximately 2% of all in-hospital deaths between 2012 and 2016; the numbers steadily increased year-over-year in the United States during that interval, from 12 575 in 2012 to 15 405 in 2016 (3). However, neuropathologic studies of individuals surviving with assisted ventilation and other life support for any length of time after clinical declaration of brain death are relatively few, especially from the modern era, and generally comprise case reports or historic series of “respirator brain” descriptions with postdeclaration intervals of 2–21 days (4–8) (Table 1). Very few examples of longer intervals (68 days, 101 days, and 20 years) exist (9–11) (Table 2).

A highly publicized case of a young woman named Jahi McMath, who was maintained on life support nearly 4½ years after a declaration of brain death, was the subject of many articles in the lay press, written while she was still in supportive care at her home, with permission and cooperation of her fam-

ily (e.g. [12]). The clinical course of this extraordinary patient was reported in detail by one of us (DAS) who was involved directly in her case, along with neuroimaging findings 9 months after brain death declaration (13, 14). After final cardiopulmonary arrest, she underwent autopsy examination.

Here we contribute, with explicit permission of her family, an analysis of Ms McMath's neuropathologic findings, albeit with relatively limited tissue sampling of the brain specimen. We humbly acknowledge our inability to correlate them with her functional capabilities so many years after formal clinical and radiologic analyses. To place our observations in context, we further offer an overview of the literature regarding known brain tissue changes in relevant settings.

## MATERIALS AND METHODS

The clinical case data are published (13, 14). Briefly, Ms McMath underwent a tonsillectomy at age 13 years, followed by bleeding complications resulting in cerebral hypoxia-ischemia and a clinical diagnosis of brain death per conventional criteria

(13). Her family declined to accept this determination, and through legal channels she was transferred to a hospital in a different state that accommodated their beliefs and values. Maintained on ventilatory and other complementary support, she eventually was able to be cared for at home, with occasional hospitalizations for infections and metabolic derangements. Neuroimaging studies were performed 9 months after brain death declaration (i.e. 3 years and 9 months prior to “somatic” death), and reported by one of us (DAS) (14). Following a final hospital admission more than 4 years after brain death declaration, she succumbed to septic and abdominal complications. Her family consented to autopsy examination, performed at Robert Wood Johnson University Hospital (RWJUH) at New Brunswick, New Jersey, which took place 60 hours later.

For this report, macroscopic photographs of the skull and brain were available from the time of autopsy at RWJUH. Sectioning of the formalin-fixed specimen, photography of the coronal sections, and sampling for neurohistology occurred some months after autopsy, at a different institution. Neither contemporaneous notes from that examination, nor “wet” (formalin-fixed, stock) brain tissue remnants were available for our independent review.

We performed microscopic analysis of 14 formalin-fixed, paraffin-embedded blocks of the central nervous system, provided with permission of the mother, Ms Nailah Winkfield, and the family’s spokesperson, Mr Christopher Dolan. These included cerebral cortex and a small amount of subcortical white matter, with adherent convexity dura, of uncertain precise neuroanatomic locations: of 9 such blocks, 2 were likely from parasagittal frontal lobe with subdural hemorrhage, as visible grossly in the available macroscopic photographs; 3 had tentorium with adherent cerebellar and occipital cortex; one had cerebellum with adherent posterior fossa dura; and one had free dura mater from an uncertain site (see “Results”). Samples of basal ganglia, thalamus, hypothalamus, hippocampus, brainstem, or spinal cord structures were not available. The paraffin blocks were cut and stained using standard protocols in the Neuropathology Brain Bank and Research Core at Mount Sinai. Hematoxylin and eosin (H&E) stains were performed on the glass slides from all blocks. Perls iron and trichrome stains, elastic-Van Gieson silver impregnation, and CD68, CD34, and NeuN immunostains were performed on selected blocks, using standard diagnostic procedures.

## RESULTS

### General autopsy findings

These were reported in detail as part of the clinical account of Ms McMath’s course and included multiorgan failure following laparotomy for recurrent pneumatosis intestinalis, retroperitoneal hemorrhage, and hepatic steatosis, with icterus, as well as diffuse alveolar damage (13).

### Macroscopic brain evaluation

The cranial vault was markedly thickened relative to that expected for age (personal observation [RDF]; ruler absent from photographs). The inner aspect of the thickened calvarium was irregular, with a “cobblestone” appearance of the

bony inner table, and adherent wisps of fibrous tissue (dura mater) and soft (i.e. nonbony) material having dark red to orange-yellow discoloration (Fig. 1A). Examination of the brain in situ after removal of the calvarium (Fig. 1B) shows a markedly abnormal extradural surface, with adherent dark red flocculent material (lower portion of Fig. 1B). The frontal lobes were disrupted by handling artifact, uncovering marked yellow-green discoloration (icterus) of the subdural surfaces, to which degenerated brain tissue, having a paste-like appearance, adhered in irregular fragments (upper portion of Fig. 1B). Once removed from the cranial vault (Fig. 1C), the brain and firmly adherent calvarial and portions of basal dura mater weighed 750 g (average expected weight for a female age 16–18 years, 1340 g [for brain only]) (15). Ventral temporal lobe, brainstem, and cerebellar landmarks were poorly visualized, owing to marked tissue fragmentation, although general outlines suggested the cerebellar hemispheres and basis pontis (arrows and arrowheads, respectively, in Fig. 1C). The surfaces of these basal structures were discolored orange-yellow (typical of old hemorrhage, present in the subdural and/or subarachnoid space). Much of the basal dura remained adherent to the skull base, and also showed marked yellow-orange discoloration of the subdural surface (i.e. evidence of old subdural hemorrhage) (Fig. 1D).

After formalin-fixation, the brain and adherent dura (Fig. 2A–C) were accompanied by several rounded gray fragments resembling diencephalon (not further sectioned, photographed, or blocked for histology). The brain/dura block was sectioned approximately in the coronal plane. As noted externally, there was artifactual disruption (related to brain removal) in several spots, including the frontal and inferior temporal lobes (Fig. 2D, E). The occipital lobes with subjacent tentorium and cerebellar hemispheres and vermis (Fig. 2F) were the best preserved and showed a clear outline of the occipital cortical ribbon and subcortical white matter and cerebellar folia (though having a dusky discoloration and unusual granular surface texture). In many foci, rusty orange-yellow discoloration affected the cerebral cortical/adherent subdural boundaries, and even within the dura, indicative of old hemorrhage. Tracking of this orange discoloration superficially into cortical sulci (old subarachnoid hemorrhage) was focally present. In addition, linear foci of dark red subdural blood were noted over the parasagittal frontal lobe surfaces (arrows in Fig. 2D). Focal red-brown material was adherent to the epidural surfaces of the parietal and occipital lobes (Fig. 2E, F), corresponding to that seen overlying the dural surface in the in situ autopsy photographs (Fig. 1B). The ventricles and periventricular white matter, corpus callosum, basal ganglia and thalamus, hippocampi, and brainstem were not identifiable on the cut section photographs.

### Microscopic brain analysis

The microscopic findings will be presented from the “outside in,” so to speak, since these more superficially located tissues were the only sites of “normal” H&E staining, and thus represented the preserved, apparently previously “viable” tissue (as expected in typical, formalin-fixed autopsy specimens, even after 60 hours’ interval). The epidural surface of the calvarial

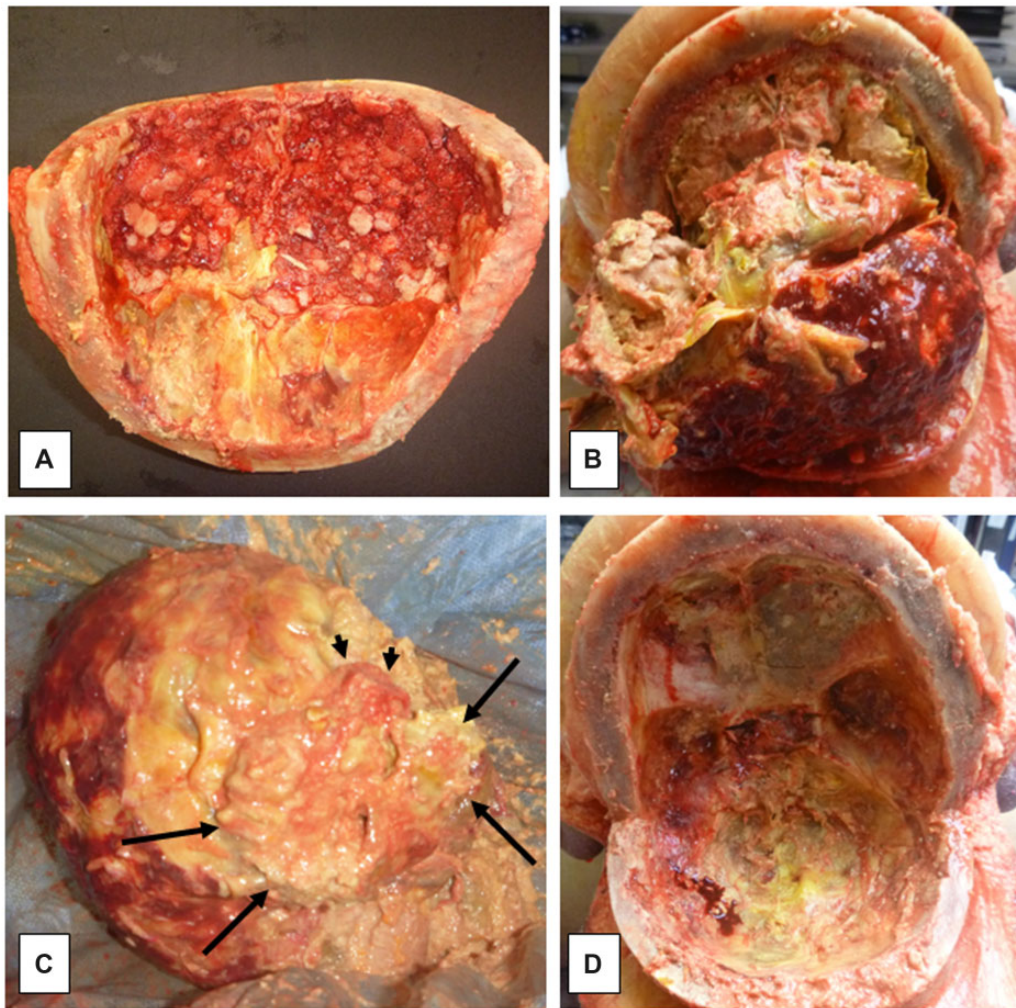


**Figure 1.** Macroscopic findings at autopsy. Inner aspect of markedly thickened and nodular calvarium (A); brain partially covered by calvarial dura mater, in situ after removal of calvarium, with artifactual (removal) disruption (B); ventral aspect of brain after removal from skull (C, long arrows demarcating the possible contours of the cerebellum, and short arrows the possible basis pontis), with artifactual (removal) disruption; base of skull after brain removal (D). (See text for additional description.)

dura mater showed a variably thick epidural layer of trilineage hematopoietic cells in fibroadipose tissue, accompanied by focal iron deposition (bone marrow metaplasia, an established form of extramedullary hematopoiesis, a phenomenon recognized to occur particularly in pediatric subjects [RDF, personal observation]) (Fig. 3). The calvarial and tentorial dura were also notable for fibrocollagenous thickening, with patchy iron deposition between the collagen fibers and associated with multifocal obliteration and recanalization of the venous sinuses (Figs. 3 [circled area], 5, and 7). Elastic-van Gieson silver preparations highlight occasional wavy elastic profiles completely filled with collagen (thrombosed dural arterioles); scattered such vessels are patent along the inner few collagen layers of the dura, in contrast to the usual more epidural localization of meningeal artery branches (Fig. 4). These patent dural arterioles, along with leptomeningeal arterioles which entered the superficial cortical sulci, tended to be associated with organizing necrotic foci of the superficial cortical ribbon (see below) (Figs. 4 and 6).

The inner aspects of the calvarial and tentorial dura mater were closely apposed (by fibrous adhesion) to the pia of the underlying cerebral and cerebellar cortices, respectively (Figs. 1–6). The calvarial dura was further notable for recent-on-subacute-on-chronic subdural hemorrhage (highlighted on iron stains and CD68 immunostain for macrophages) (Figs. 3 and 6). Hemophagocytosis, indicating recent hemorrhage of at most 24–72 hours prior to demise, and corresponding to Ms McMath agonal systemic bleeding diathesis, was clearly present (Fig. 8). At these points of dural/cortical adherence, the molecular layer and focally layers 2–3 of the cerebral cortex had coarsely grouped mineralizations, as well as focal intraparenchymal recent-on-subacute-on-chronic hemorrhage, contiguous with the subdural hemorrhagic foci (Figs. 2, 5, and 8). Some of these adherent cortical zones had fibrin deposition and macrophages suggesting organizing necrosis/hemorrhage (Fig. 8).

The available H&E sections including cerebral and cerebellar cortex and subjacent white matter all showed pallor and

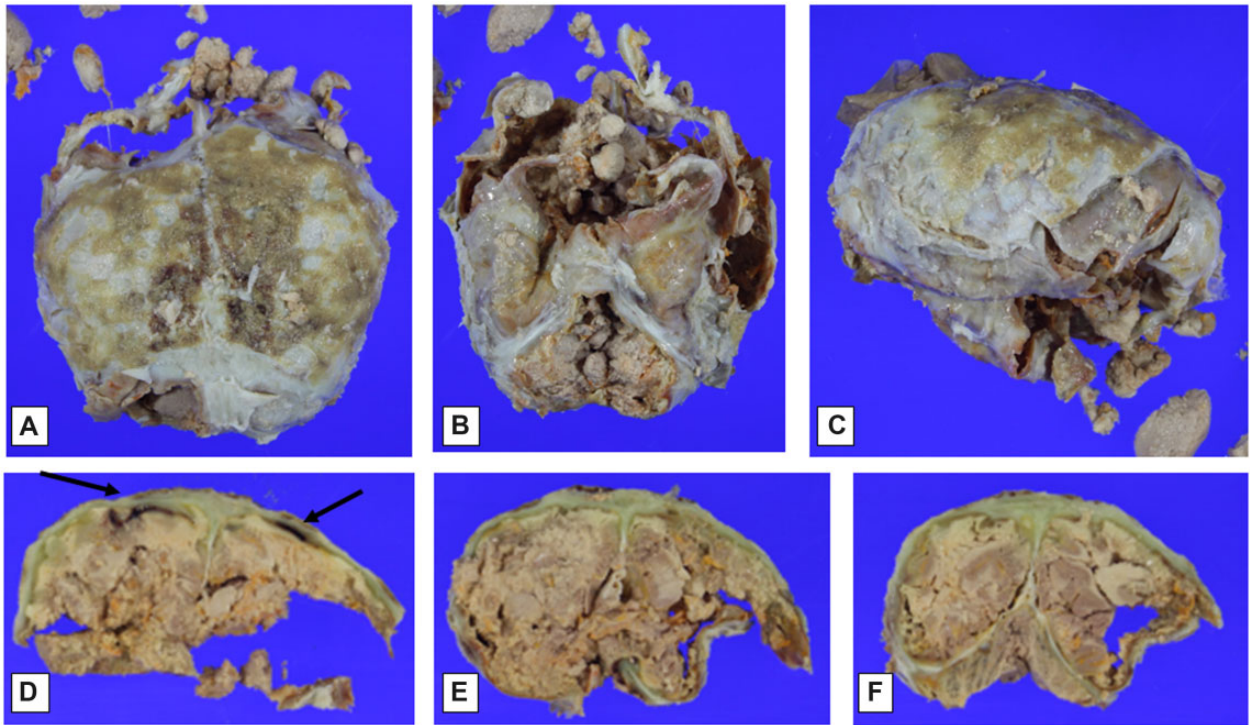


**Figure 2.** Macroscopic findings at time of formalin-fixed brain evaluation. Dorsal view of brain covered by adherent calvarial dura mater and epidural tan-brown granular material (A); frontotemporal view of brain partially covered by dura mater (brainstem and cerebellum indistinct) (B); lateral view of brain and dura (side uncertain) (C); coronal section of posterior frontal cerebral hemispheres and adherent calvarial dura mater, showing bilateral red-brown subdural discoloration (arrows), as well as possible dural icterus (green discoloration), and with focally discernible tan-brown cerebral cortex overlying tan white matter, with focal yellow-orange foci (D); coronal sections at parieto-occipital and occipital/cerebellar levels (E, F), with similar changes to those seen in panel (D). (See text for additional description.)

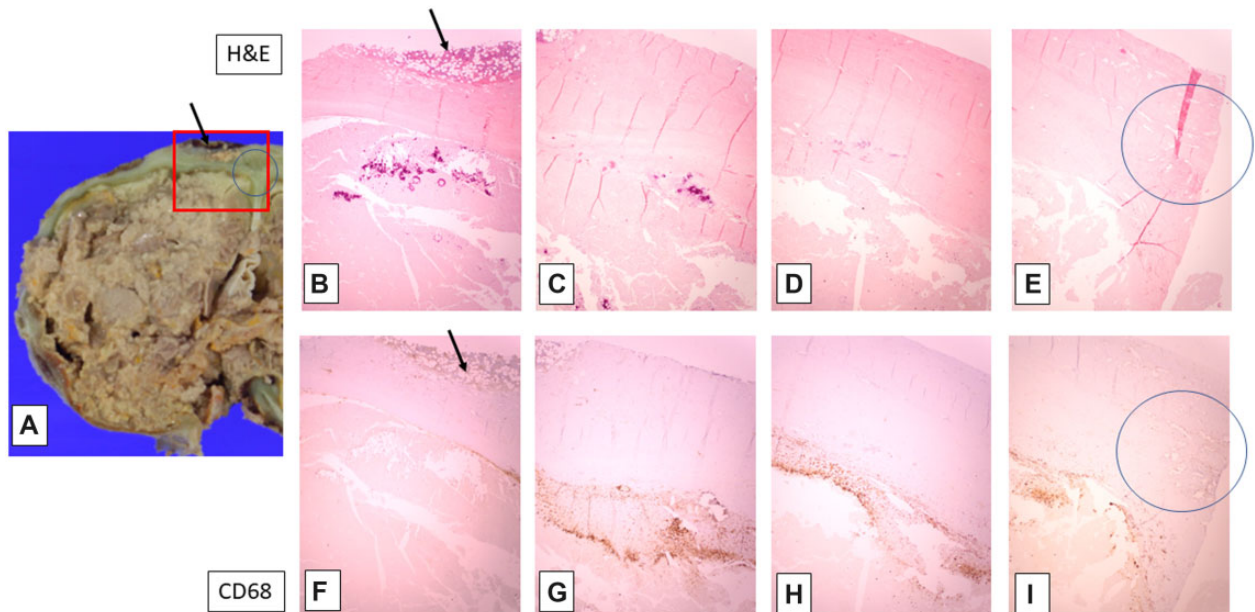


**Figure 3.** Gross and microscopic findings in the left posterior frontal cortex. Left cerebral hemisphere cortex with adherent dura (top, A), and serial fields from left (lateral) to right (medial) within red-boxed area (all, original magnification: 20 $\times$ ); note epidural bone marrow (arrows in A, B, F), dural venous occlusion and recanalization (circles in A, E, I), and calcification (magenta deposits in B and C) with macrophages (CD68 [brown] immunostaining in F-I) in partially reperfused superficial cortex. (See text for additional description, and subsequent figures for higher magnifications.)

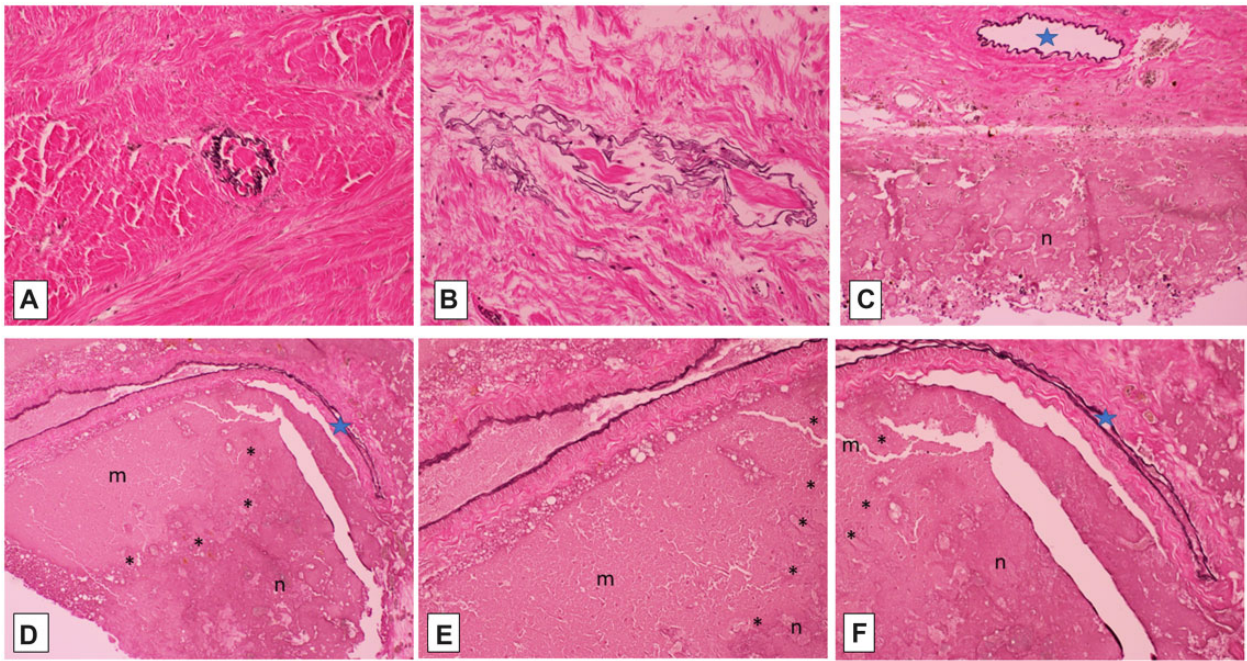


**Figure 4.** Elastic-van Gieson silver impregnations, showing dural arterioles completely occluded by collagen, as outlined by black elastica remnants (A, B; 200×); focally patent dural (C, 100×) and penetrating intrasulcal (D, F; 100×) arterioles (blue stars) are associated with necrosis (n) of subjacent cerebral cortex (C–F), delineated by asterisks (\*) from adjacent nonviable mummified cortex (m) (D–F; E, 200×).

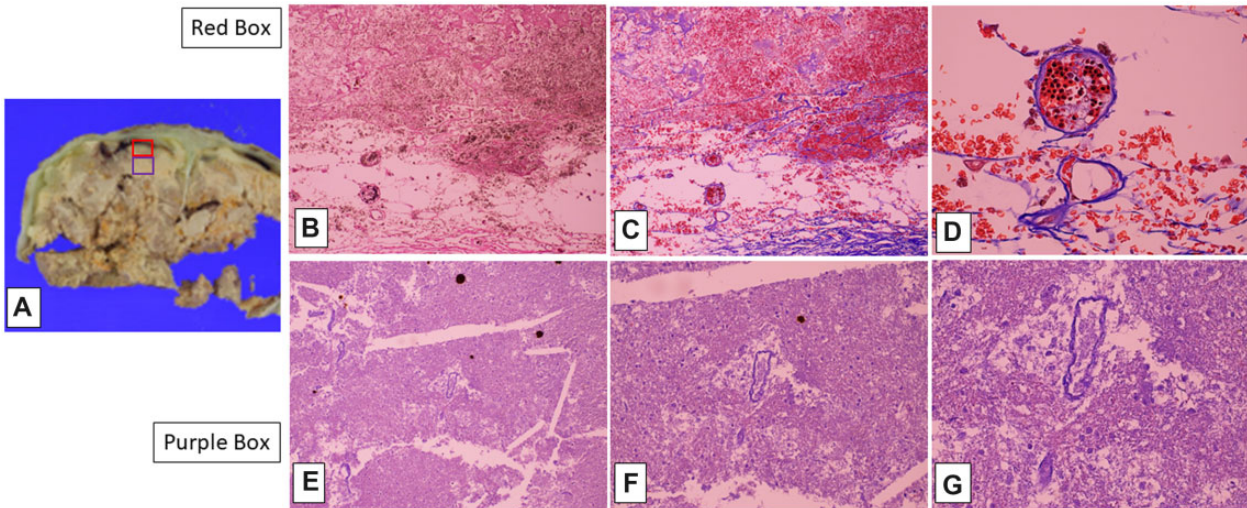


**Figure 5.** Difference between superficial parietal cortex at site of submeningeal hemorrhage (viable) (red box in A; B [elastic-van Gieson]; C and D [Masson trichrome]) and subjacent cerebral parenchyma (mummified) (purple box in A; E–G [Masson trichrome]). Note old hemorrhage (brown hemosiderin, B [40×]) and intact red blood cells in fresh hemorrhage and within microvascular lumina, along with terminal circulating white blood cells (C [40×] and D [200×]), in contrast to lack of intravascular intact red blood cells in deeper mummified parenchyma lacking cellular reaction (E [40×], F [100×], G [200×]).

total loss of hematoxylin staining of nuclei, although faint eosinophilia outlined recognizable neurons, glial cells, parenchymal and meningeal vessels (a histopathological appearance variably referred to in both human and veterinary medical literature), depending on the context, as “autolysis,” “maceration,” “mummification,” and “adipocere formation (saponification)” which can remain many years after death (discussed further below) (Figs. 4–6, 8, and 9) (16–19).

Aside from this staining pallor, the brain parenchyma maintained relatively preserved architectural relationships between cortical ribbon and immediately subcortical/intragyrus white matter. The superficial cortical layers were disrupted focally by dystrophic cortical mineralization (so-called “droplet” mineralization, seen as purple-blue dots on H&E, and with pale positivity on iron stain) at points of dural adherence (see below) (Figs. 6 and 8). There were scattered pale, fluffy crys-

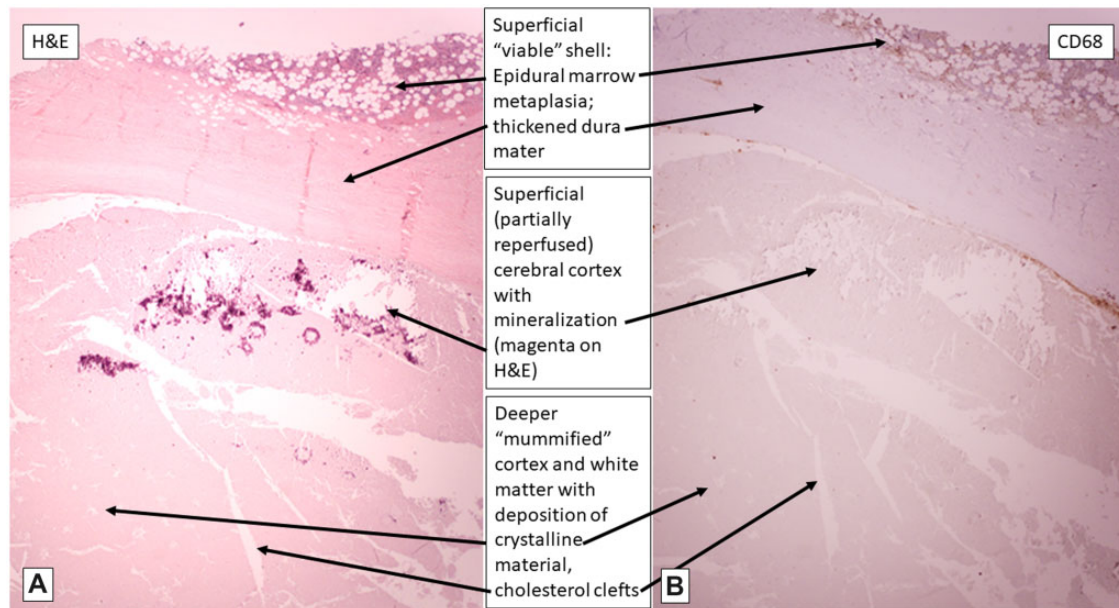


**Figure 6.** Detail of microscopy of posterior frontal cortex and adherent dura mater (A, H&E, 20 $\times$ ; B, CD68 immunostain for macrophages, 20 $\times$ ).

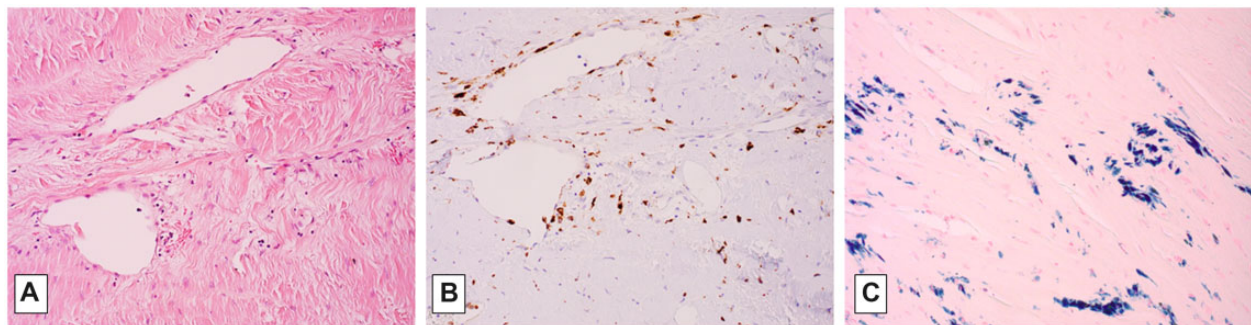


**Figure 7.** Calvarial dura and venous sinus with collagenous occlusion and recanalization (A, H&E, 200 $\times$ ); macrophages in collagenized lumen (B, CD68 immunostain, 200 $\times$ ); and hemosiderosis (C, iron stain, 200 $\times$ ).

talline deposits in the cerebral and cerebellar cortices and subcortical white matter (Figs. 4–6, and 8). Note that these phenomena are seen in the setting of macerated stillbirth, “mummification,” and adipocere, and are considered postmortem/prefixation artifacts, related to autolysis at body temperature, without blood flow to allow for arrival of inflammatory cells and removal of dead tissue by macrophages, as would be seen otherwise in liquefactive necrosis (personal observation, RDF and JFC) (16–19). In addition, variably sized needle- or lens-shaped spaces, consistent with cholesterol clefts (as often seen in settings of nonspecific cellular membrane breakdown, such as in old cerebral infarcts or degenerative lesions (20)), were evident in the subcortical white matter (Figs. 4–6, and 8) and depths of cerebellar cortex.

In areas, macrophages were identifiable (confirmed on CD68 immunostain) concentrated at sites of recognizable necrosis, e.g. in the cortex just beneath the adherence to dura (Figs. 3 and 6) and in the epidural focus of marrow metaplasia (Fig. 3).

Multifocal deposition of bilirubin crystals was noted, generally in regions of the recent-on-subacute-on-chronic hemorrhage in the superficial cortex (Fig. 8), corresponding to macroscopically visible yellow-orange discolorations, likely including those present in deeper cerebral tissues (though these were not sampled for histology) (Figs. 1–3, 8, and 9).

Additional immunostains for vascular cells (CD34) and neurons (NeuN) were negative, even in relatively well-fixed tissues, suggesting technical failure, perhaps related to prolonged fixation or embedding affecting these particular antibodies, considering that other immunostains were adequate.

Importantly, no “Swiss cheese” artifact (postmortem putrefaction due to anaerobe overgrowth, a phenomenon often seen in postmortem intervals greater than 24 hours) was identified in the available sampled locales. There was no evidence in any section of brain parenchymal vascular endothelial reactive changes, prior old cortical laminar necrosis, or cavitation with tissue dissolution, as would be seen, even after many years, in arterial territory infarcts.

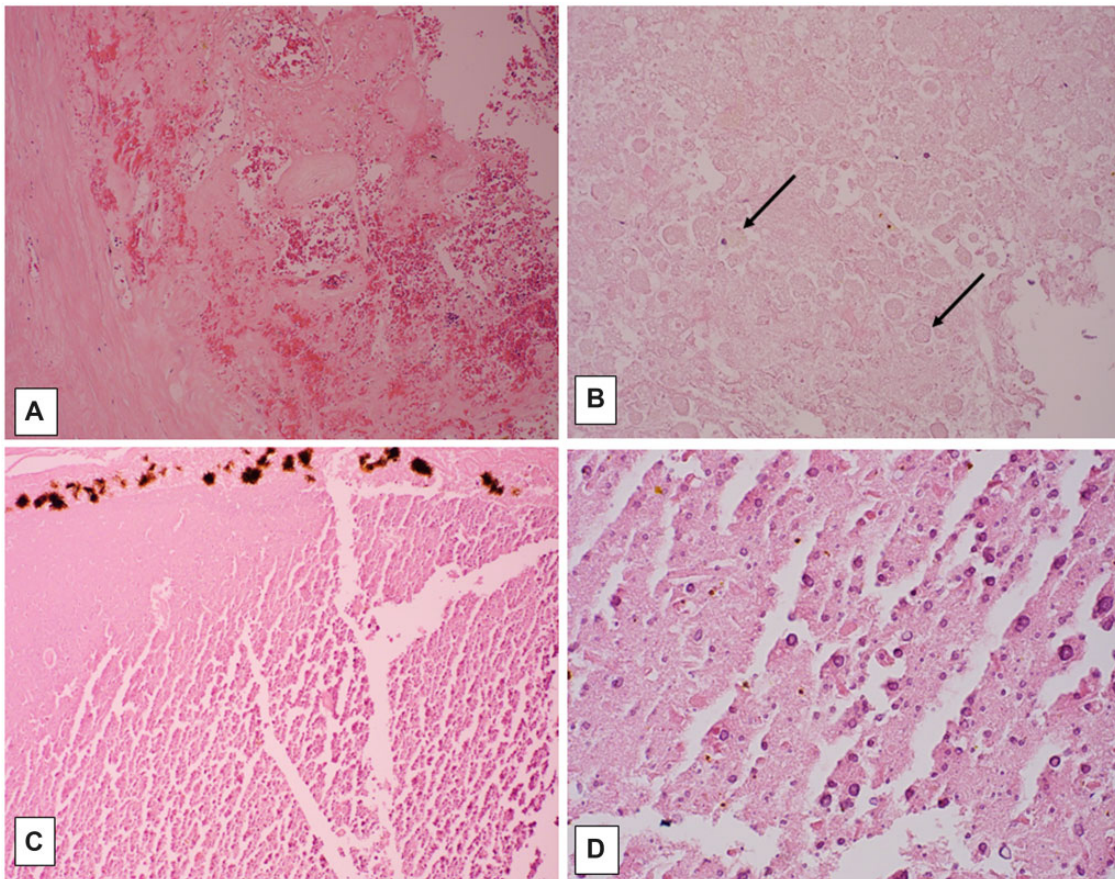


**Figure 8.** Cerebellar cortex with recent hemorrhage (visible as intact red blood cells) and fibrinous reaction along subdural aspect (**A**, H&E, 100×), with hemophagocytosis (older, organizing hemorrhage) visible in “ghost-like” macrophages (arrows) in deeper tissues (**B**, H&E, 200×). Superficial cerebral cortex with bilirubin crystals in molecular layer (**C**, H&E, 100×) and droplet mineralizations in deeper cortical layers (**D**, H&E, 400×). Note “ghost-like” neuronal outlines between calcifications in (**D**).

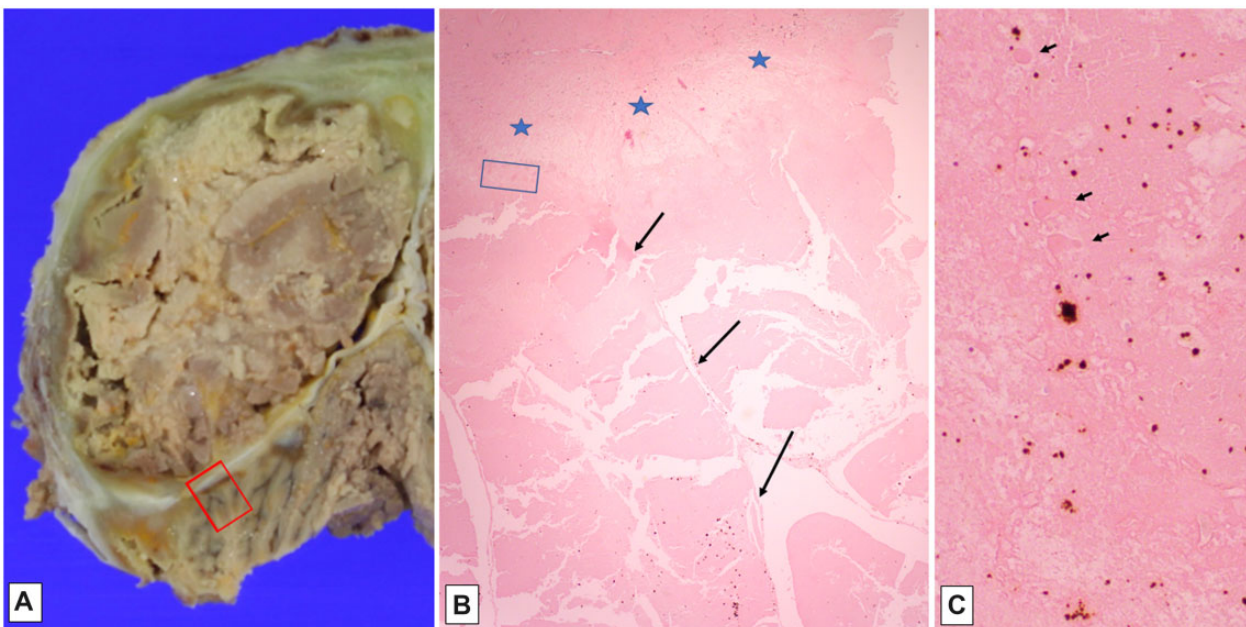


**Figure 9.** Gross fibrous adherence of tentorium to overlying occipital cortex and underlying cerebellar cortex, with yellow-orange discoloration (**A**); histologic section (**B**, H&E, 20×) of red-boxed area in (**A**), showing subpial molecular layer adherent to tentorium (delimited by blue stars), and underlying autolyzed cerebellar cortical folia (long arrows) with cholesterol clefts and artifactual cracking of tissue; blue-boxed area in (**B**), showing “ghost-like” Purkinje cell profiles (short arrows), as well as orange-brown bilirubin crystals (**C**, H&E, 200×).

**Table 1.** Neuropathology reports among brain death cases following relatively short intervals

Reference	Ages	Interval	Neuropathology	Interpretation
Grunnet and Paulson, 1971 (4) (n = 17)	2 mo to 60 y	1–7 d (single case of 21 d “requiring a respirator only intermittently”)	“Fourteen had no inflammatory, microglial, or endothelial response”; “several also showed few perivascular neutrophils or lymphocytes in the brain stem”; “three [with] . . . inflammatory response” had “onset of disease [that] had been relatively slow” (requiring “a respirator. . . more than a day after the neurological insult”)	Fourteen without tissue response represented “in vivo autolysis,” due to “inadequacy of blood supply . . . through rapidly developing and severe cerebral edema.” “There is no more opportunity for active inflammation to occur than in the autolyzed brains seen when postmortems are done several days after death.”
Walker, 1975 (5) (n = 226)	>1 y	12 h to 7 d	“Respirator brain,” 40% (especially after 24–48 h) with “little or no inflammation”	“certain changes are almost indistinguishable from the postmortem alterations resulting from delayed fixation or after storage of the cadaver . . . over 90°F”
Pearson, 1977 (6) (n = 13)	NS	20 h to 5.5 d	Those <i>with</i> detectable radioisotope bolus had reactive changes; Those <i>without</i> had “autolysis” = “tissue breakdown that is dependent on intrinsic cellular enzymes and independent of factors derived from flowing blood” “ghostlike changes” of neurons, “lysed red cells” in vessels	Avoided term “respirator brain . . . [as] it is not the presence of a respirator but the absence of major intracranial blood flow which is associated with brain death and autolysis”; “blood may persist in preexisting hemorrhages or in vessels congested at the time circulation ceases”
Schroeder, 1983 (7) (n = 190)	8 mo to 75 y	1 h to 13 d	“neuronal necroses. . . arise at different rates within the cerebral cortex and the lower brainstem”; development of “washed-out tissue picture”	“hemorrhages and . . . necroses in some cases with longer intervals. . . [suggest incomplete] cerebral ischemia”
Wijdicks and Pfeifer, 2008 (8) (n = 41)	19–80 y	0–36 h	Neuronal ischemia “no inflammatory or cellular reaction”	“total brain necrosis not observed”

Interval refers to interval on cardiorespiratory support following clinical interpretation of irreversible brain injury (brain death). d, days; h, hours; min, minutes; mo, months; N, number of cases in report; NS, not stated; y, years.

## DISCUSSION

### Brief overview of concept of brain death

One of the first observations of apparent brain death was uncovered among the writings of Harvey Cushing (from 1908, as published by Pendleton et al [21]), following intraoperative cessation of respiration and implementation of artificial respiration (by use of a manual bellows through a tracheal stoma), and later surgical decompression via a “cranial window,” until subsequent “cessation of all cardiac activity” supervened after 36 hours. Cushing went on to describe the “perfectly anaemic brain. . . of a gray, colorless appearance, broken only by the black, greatly distended veins” that herniated from the cranial defect. Subsequent clinicopathologic observations notably included initial descriptions by Aldarete et al (22) of a cohort of patients “in irreversible coma. . . [with] fixed, dilated pupils, no reflexes, no movements, and no spontaneous respirations, and a flat isoelectric electroencephalogram.” Neuropathologic findings were summarized among 80 examined cases as showing “damage ranging from total liquefaction, where microscopic structure was not identifiable, to brains with islands of relatively normal cortical structure.” The term “Brain-Death Syndrome” as a type of “hypoxic panencephalopathy” was first used by Adams and

Jéquier (23) the following year (1969), who highlighted the ethical issues of defining the moment of death as “irreversible cerebral damage,” instead of cardiorespiratory cessation by bedside determination, in the modern era of “artificial means” of life support. Key literature accounts of detailed neuropathologic features of brain death are collated in Tables 1 and 2.

### Neuropathologic diagnoses

The final neuropathologic diagnosis is outlined in Table 3 and summarizes our conclusions based on the available macroscopic photographs and neurohistology, given the clinical context. The organization of the diagnosis follows the principles used in classical autopsy reporting, that is, to describe observed phenomena in objective and accepted pathological terms, while offering the interpretation (here labeled “consistent with”) that best encompasses and explains all available findings, resting in turn on the medical literature and on extensive personal experience in brain analysis of living (biopsied) and dead (autopsied) individuals (RDF and JFC). We emphasize that the limited amount of tissue sampling, in particular the lack of blocks from the diencephalon, brainstem, and spinal cord for microscopic analysis in this case, places constraints on our ability to infer any correlation with central nervous system

**Table 2.** Neuropathology reports among brain death cases following long intervals

Reference	AgeInterval	Neuropathology	Interpretation
Parisi, 1982 (9) (n = 1)	49 y 68 d	Transverse dural sinus thrombosis; cortical subpial vascularization and macrophages; “coagulative necrosis but . . . no evidence of cellular reactivity” of deeper structures	“Inward progression of the reparative response from the leptomeningeal surface, presumably originating from the intact extracranial circulation”
Ito, 1992 (10) (n = 1)	14 y 101 d	“Proliferation of vessels and fibrosis. . . [and] erythrocytes, leucocytes and scavenger cells in the dura mater”	“Secondary petechial haemorrhage. . . appear to occur long after the trauma, in spite of the complete cessation of cerebral blood flow . . . [and] may be produced from newly formed vessels in the dura mater by secondary circulatory disturbances” . . . [since] the blood flow of the dura is maintained by the middle meningeal artery which originates from the external carotid artery
Repertinger, 2006 (11) (n = 1)	4 y 20 y	Calcified shell, with ossification and marrow, grumous mummified material, mineralized cell processes, iron pigment, extensive small focal calcifications	“blood flow was insufficient over the 2 decades for macrophages to arrive and remove most of the debris”

d, days; n, number of cases in report; y, years.

**Table 3.** Final neuropathologic diagnoses based on available macroscopic photographs and paraffin blocks

I. (History of global cerebral hypoperfusion following therapeutic tonsillectomy at age 13, subsequently meeting clinical “brain death determination” guidelines, followed by maintenance on life support measures for 4½ years):
A. Portions of brain with:
i) Widespread autolysis (resembling “mummification,” “saponification”), with acellular degenerative changes, of deep cerebral and cerebellar cortex and white matter, consistent with near-total absence of perfusion and reperfusion;
ii) Focal partial revascularization of superficial cerebral and cerebellar cortices, with microscopic macrophage infiltrates, mineralization, old and recent microhemorrhage, consistent with old hypoxia-ischemia and limited reperfusion, apparently from dura mater (external carotid and vertebral arterial blood flow).
B. Portions of dura mater with:
i) Obliteration and recanalization of venous sinuses;
ii) Intradural iron deposition, consistent with old hypoxia-ischemia and reperfusion;
iii) Fibrous adhesion of convexity and tentorial meninges to superficial cerebral and cerebellar cortex;
iv) Recent-on-subacute-on-chronic submeningeal hemorrhage, with focal extension into superficial cerebral and cerebellar cortices;
v) Thick epidural extramedullary hematopoiesis (marrow metaplasia);
vi) Focal autolysis (resembling “mummification”, “saponification”).

functionality during the interval following declaration of brain death and final “somatic” death years later. In particular, the fascinating clinical observation of apparent onset of menses suggests at least some element of preservation of the hypothalamic-pituitary axis, the basis of which we cannot confirm. Moreover, ascribing any histologic appearance in the autopsy specimen to the clinical stroke- or trauma-related phenomenon of “ischemic penumbra” (defined as an area of

decreased perfusion too low to support function but high enough to prevent necrosis), whether it may have been part of the neuroimaging picture at any time after brain death declaration, is not possible at this point (24–26). Reasoning further, we refrain from discussion of the various disorders of consciousness as they are beginning to be understood and defined, and of the ethics attendant to these issues (27–29), as they are beyond the scope of this paper.

### Concept of extra- to intracranial revascularization

Our interpretation regarding the likely extracranial revascularization of the superficial (submeningeal) brain tissue, where necrosis and reactive changes are seen, is based on established observations of external-to-internal cerebral vascularization, performed therapeutically in cases of Moyamoya disease, for example (30) (see diagrammatic representation of this concept in Fig. 10). In this surgical procedure, blood flow is partially restored to chronically and progressively ischemic brain regions (resulting from postradiation or idiopathic leptomeningeal arteriolar narrowing) by routing of the middle meningeal artery through the dura to the underlying arachnoid, so as to effect a degree of cortical revascularization. Very few neuropathologic accounts of the results of this procedure are available in the literature; however, one such case autopsied 20 years after the external-to-internal revascularization documented that “countless meandering vessels on the internal surface of the dura mater connected with small vessels on the brain surface and in the subpial brain tissue” (31). Not depicted in our schematic diagram is the likely origin of reperfusion of the similarly relatively preserved superficial occipital and cerebellar cortices (seen in our Figs. 4 and 9) from meningeal branches of the vertebral and/or ascending pharyngeal arteries which normally supply the posterior dura mater.

In Ms McMath’s case, while the some of the dural arterioles were completely occluded by collagen (organized thrombus), some remained patent, and, although demonstration of direct connection between extradural arteries and penetrating corti-

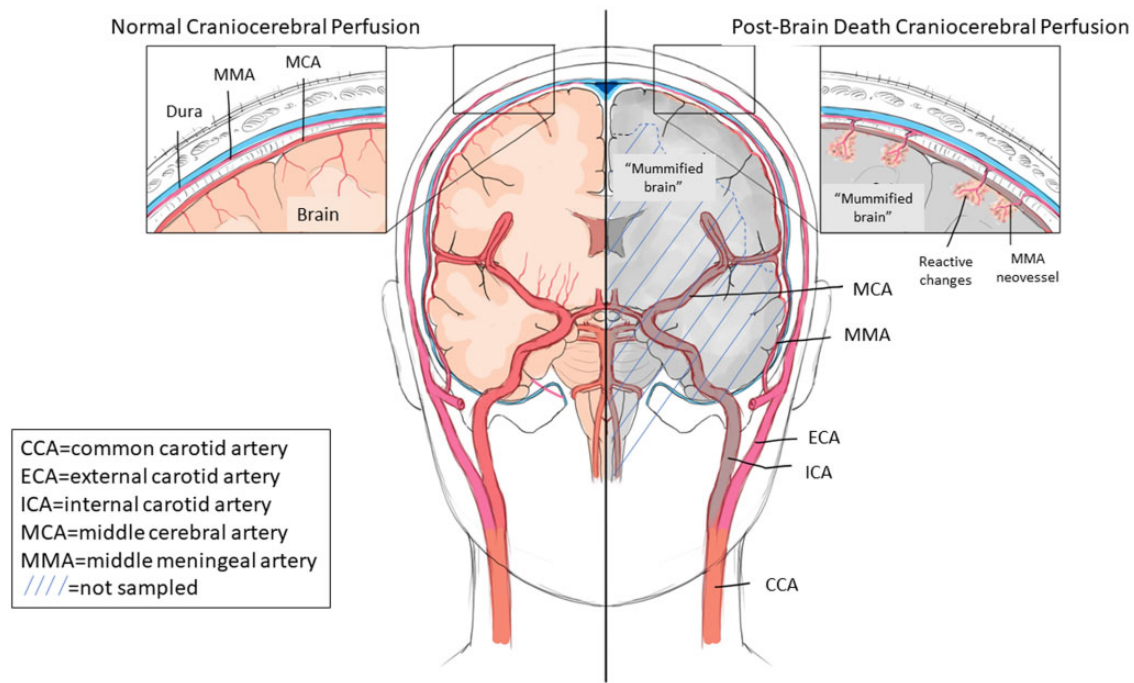


**Figure 10.** Diagram of normal craniocerebral perfusion (red-colored vessels on left) and presumed spontaneous external-to-internal carotid reperfusion (red-colored vessels on right), following (sub)total interruption of internal carotid artery perfusion (gray-colored vessels on right) at time of declaration of brain death, and permitting focal cellular reactive changes in superficial cerebral and cerebellar cortices by neovessels branching from middle meningeal artery (right, and inset). CCA, common carotid artery; ECA, external carotid artery; ICA, internal carotid artery; MCA, middle cerebral artery; MMA, middle meningeal artery. Insets, higher-power representation of normal (left) and modified (right) perfusion of superficial cerebral cortex. Hatched area denotes brain regions not sampled for neurohistology. An analogous revascularization phenomenon to the occipital and cerebellar cortices is postulated to have occurred from those regions of dura mater supplied by branches of the vertebral and posterior pharyngeal arteries (not depicted). For detailed description of reactive changes (inset, right), see text.

cal vessels is not reliable in tissue sections, the observation of arterioles extending along gyral crests and into cortical sulci and their geographic localization to areas with clear evidence of necrosis and reactive changes (macrophages, mineralization, old and even recent hemorrhage) is compelling. Conversely, the regions without such intact vasculature, including the deeper cortical layers and subcortical white matter, were the ones that showed an autolytic picture (as diagrammed in Fig. 10; discussed further below). Of note, the presence of hemosiderin and recent hemorrhage in some of these areas may be sequelae of hemodynamic fluctuations, ongoing minor trauma, and/or periodic/agonal coagulopathy. The dural venous channels had clear-cut evidence of collagenous occlusion and recanalization, considered related to stasis of venous flow following the global decreased cerebral (arterial) perfusion (illustrated in our Figs. 3 and 7).

#### Brain tissue viability as inferred by autopsy

The histologic findings of faintly stained outlines of neurons and other cells raise the obvious question: Were these “viable” before our young woman’s “somatic” death? To address this question, we need to understand what is meant by the terms “viable,” “necrotic,” and “autolyzed” (the latter also relating to the concepts of postmortem tissue changes variably referred to as “mummification,” “maceration,” and “saponification”), as well as “decomposition” (or “putrefaction”) as used among

pathology specialists in several relevant contexts (Table 4; Figs. 11–13). “Viability” and “necrosis” as used in neuropathology derive from widely established appearances, both macroscopic and microscopic, of surgically resected tissues having short, known intervals between removal and processing (fixation). As such, these features are the “closest” an observer can be to what is happening in the tissues of the patient. All of medicine relies on this time-honored means of diagnosis by pathologists for treatment and understanding of human disease. Thus, “viability” is denoted by the typical nuclear basophilia and cytoplasmic eosinophilia (e.g. as visible in Fig. 7A), corresponding by convention to integrity of cellular structures. “Necrosis” is characterized by nuclear pallor and eventual fragmentation, and in perfused conditions, is accompanied by microvascular reaction (endothelial and pericyte prominence and proliferation), inflammatory infiltrates and phagocytosis; over time, gliosis, cavitation, and sometimes focal “mummification” result, and can be present for many years after the inciting event, including in old infarcts and contusions (personal observation [RDF and JFC]). If there is no perfusion whatsoever (i.e. in areas of the brain in “brain death” in which a clinically administered bolus of radioisotope is not detected), there can be no microvascular reaction, inflammation, or phagocytosis of devitalized cells (Table 1; Fig. 11) (6). This appearance was interpreted by Grunnet and Paulson (4) as a process of “in vivo autolysis,” resulting from the

**Table 4.** Definitions of tissue changes relevant to brain death analysis

Process	Definition	Histologic Hallmarks	Reference
Viability	Perfused and oxygenated tissue at time of sampling (biopsy), or up until death (autopsy), based on conventional tissue fixation and histopathologic processing; “cells placed immediately in fixative are dead but not necrotic”	Retention of cellular including nuclear detail, and architectural relationships within a tissue or organ (until altered by autolysis; see below)	(38)
Necrosis	Primary type of cell death in a tissue or organ that has undergone irreversible injury	Loss of nuclear staining and eventual cell breakdown, as a progressive process resulting in “coagulative” or “liquefactive” necrosis (e.g., infarcts, abscesses, contusions, radiation injury); evolution of changes including hemorrhage/iron deposition, reactive cell influx, and phagocytosis, and glial scar or cavitation	(38)
Autolysis (including subtypes below)	“Breakdown of cells or tissues through the release and/or deregulated activation of endogenous proteolytic enzymes,” in part dependent on ambient temperature	“Cracking along . . . surfaces and irregularities in . . . tissue density”; “nuclear chromatolysis”; “in spite of fairly advanced autolytic fragmentation, the microscopic detail of [brain] cells can be remarkably intact”	(32)
– Mummification	“Dehydration and desiccation of soft tissues. . . [in] hot and dry climates,” but may also occur “indoors. . . [and] underwater. . . [in] an acidic and anaerobic environment”	Appearance of “mummified” remains in clandestine or unwitnessed scenes some weeks or months after death; retained (macerated) stillbirth; relative preservation of architectural relationships, but loss of nuclear staining; relative stability over time, if conditions maintained	(35, 36)
– Maceration	“Softening of a solid by action of a liquid”	Liquid contributes to the degeneration of devitalized tissue, as in retained stillbirth	(32)
– Saponification	“Modification of the putrefaction process, which involves hydrolysis and hydrogenation of fatty tissues into a . . . wax-like substance. . . consisting mainly of palmitic, oleic, and stearic fatty acids”	Requires “a warm, moist, and humid environment”	(18, 37)
Putrefaction	Tissue breakdown by postmortem overgrowth of bacteria present in the body at time of death	“Swiss cheese” artifact of gas-forming bacteria; “nuclear fragmentation . . . and eventual loss of hematoxyphilia in the nuclei and Nissl substance”	(32)

Note that these changes may have overlapping features in a given circumstance. See [Figures 11–13](#) for examples.

“inadequacy of blood supply. . . through rapidly developing and severe cerebral edema”. In such regions, faint preservation of cell and nuclear outlines, including vessels containing red cell contours, is the norm. In many ways, this appearance is analogous to that seen in the retained (“macerated”) stillbirth, the brain of which is often the last to disintegrate even at maternal body temperature for prolonged periods, remaining evaluable histologically ([Table 4](#)) (personal observation [RDF]; [[32–34](#)]). Consequently, in stillbirth the term “necrotic” is not used for this appearance, acknowledging that the fetus was “viable” before the intrauterine demise (whatever its underlying reason). In this setting, the term “mummification” may be applied, particularly referring to a prolonged period of retention in utero; here, anatomic relationships may be relatively well preserved and even amenable to radiographic delineation of cortical ribbon from deeper tissues ([34](#)). “Mummification” is also used in the forensic setting to describe preservation by desiccation, in bodies in dry environments ([Table 4](#); [Fig. 12](#)). Histologically, the rehydrated tis-

sue may have pale staining characteristics, but relative preservation of cellular architecture.

The process of “saponification” is considered another type of postmortem alteration somewhat akin to mummification, but resulting instead from a relatively sterile, moist environment, with formation of a “waxy” or soap-like substance known as adipocere ([Table 4](#); [Fig. 13](#)) ([17, 18](#)). Chemically, the fatty acids of tissues undergo alteration to salts, which precipitate and remain stable for many years (even decades, if not millennia) ([16, 35](#)). Our interpretation of the finding of fluffy crystalline aggregates in the brain tissues is consonant with this idea.

Regarding the general term “decomposition” as used in autopsy settings, a more accurate designation is “putrefaction,” which is invasion and breakdown of tissues by postmortem overgrowth of commensal bacteria from the skin and aerodigestive organs, especially in unrefrigerated conditions over many hours or days ([Table 4](#)) ([32](#)). Environmentally derived fungi, insects, or animals may contribute as well, although in circumstances quite distinct from those considered here. Given the lack of such

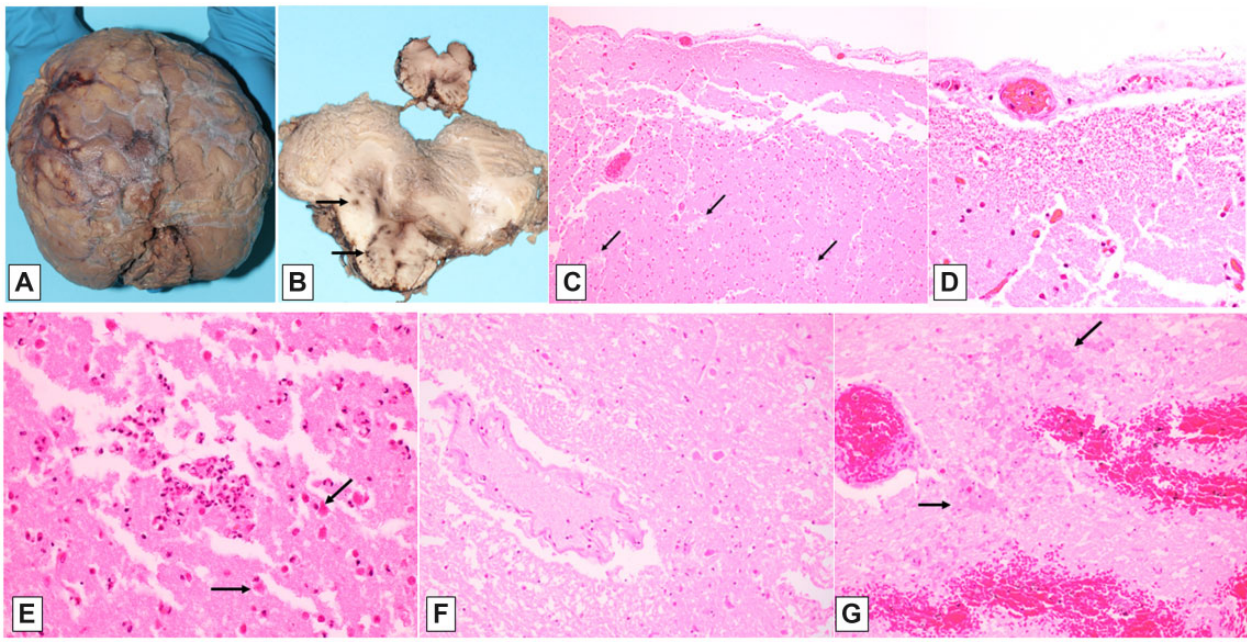


**Figure 11.** Example of macroscopic and microscopic features of brain death. Brain from a 33-year-old man with a history of sepsis, extubated 5 days following brain-death declaration, with marked swelling and gray-brown discoloration (A); note relative preservation of architectural relationships on axial cut section, as well as focal petechiae at sites of partial reperfusion (arrows, B). Neurohistology of frontal cortex, with artifactual “fracturing” of devitalized tissue; note stellate crystalline change (arrows, C; 100 $\times$ ), and finely granular subpial mineralization (D; 400 $\times$ ). Temporal cortex with artifactual “fracturing” of devitalized tissue; this area must have had partial reperfusion to allow neutrophilic influx among hyper eosinophilic (ischemic) neurons (E; 400 $\times$ ). Pons days following brain-death declaration, with “washed out picture” of devitalized tissue, and no cellular reaction; note red cell outlines visible in vascular lumen (F; 200 $\times$ ); ventral subpial region which must have had partial reperfusion to allow inflammatory cell influx (now “washed out,” arrows, G; 200 $\times$ ), and reperfusion hemorrhage (site of petechiae in B).

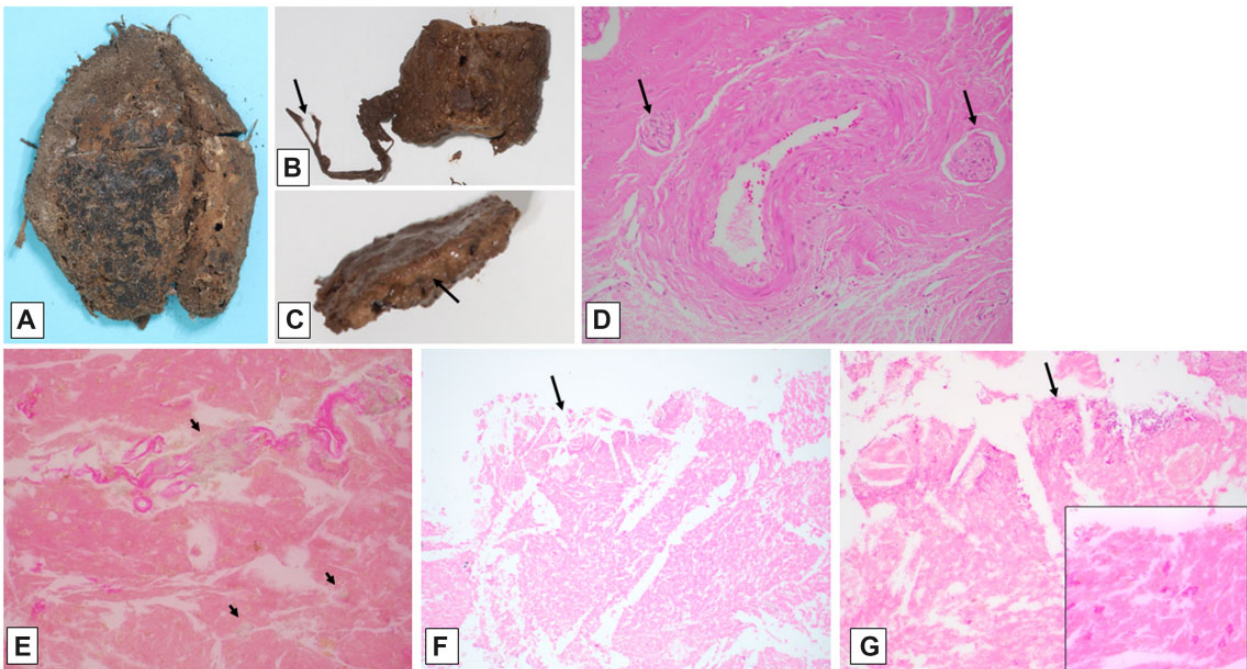


**Figure 12.** Example of macroscopic and microscopic features of tissue changes in postmortem mummification. Brain and meninges from an adult found in apartment months after last seen alive, with identifiable cerebral hemispheres (A, dorsal view), visible dura (arrow, B), and suggestion of cortical ribbon, with yellow-brown discoloration (arrow, C). Histology of mummified dura with nearly complete retention of architecture and staining quality of dural fibroblasts, vessels, and nerves (arrows, D; 200 $\times$ ). Neurohistology of leptomeninges and vessels with fluffy crystalline changes (arrowheads) in underlying cortex which also shows left-like spaces (E; 400 $\times$ ). Cerebral cortex, with lack of hematoxylin staining, left-like spaces, and punctate subpial mineralization (arrows, F; 100 $\times$ , and G; 600 $\times$ ); mineralized angular structures consistent with neurons (inset, G, 400 $\times$ ).

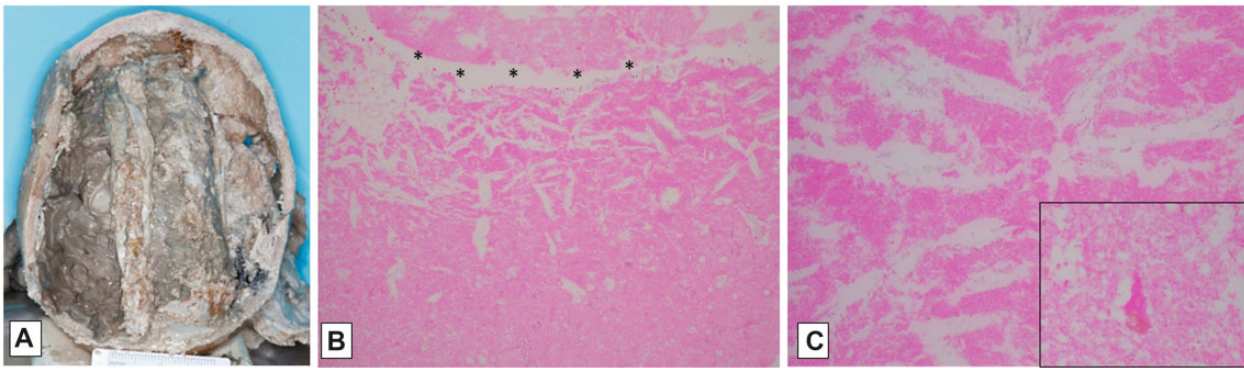


**Figure 13.** Example of macroscopic and microscopic features of tissue changes in postmortem saponification. Dorsal view of brain and dura in situ (**A**) from an adult found encased in concrete in a clandestine burial, 6 months after last seen alive, with adipocere formation; note “waxy” change of tissues, and relative preservation of cerebral gyral pattern, beneath partially reflected dura mater (left side of image, **A**). Neurohistology of cerebral cortical surface (denoted by \* in **B**) of adipocere brain, characterized by left-like spaces and stellate crystalline formations in a fine granular eosinophilic background (**B**, 100 $\times$ ; **C**, 400 $\times$ ); note distinct pyramidal neuron containing cytoplasmic lipofuscin (inset, **C**; 600 $\times$ ).

systemic changes at autopsy, and the absence of collections of bacteria on microscopic examination, it is reasonable to accept that the observed brain changes do not reflect putrefaction.

Finally, in making some of these distinctions, the macroscopic appearance of the brain plays a key role. In this case, the macroscopic brain photographs show discoloration and surface textural changes highly similar to those seen in macerated (“mummified”) stillbirth brains, as well as in brain samples from decedents whose entire bodies have undergone “saponification” (or “adipocere formation”) in certain warm, moist conditions (17). Of course, in this instance only the devitalized brain tissue was subject to one or more of these autolytic processes, within an intact skull during continued “somatic” cardiorespiratory support.

### Consideration of findings in context of reported brain death neuropathology

Despite the relatively frequent occurrence of declaration of brain death (3), the literature contains few dedicated neuropathologic reports, especially of individuals maintained for more than a few days on cardiorespiratory support. Reported cases of short intervals (up to 2–3 weeks) after brain death declaration give us insight into the initial tissue reactions (or lack thereof) after interruption of cerebral perfusion (Table 1) (2, 4–8). Analyses of these types of cases emphasize the relative lack of any tissue reaction (i.e. neutrophil and later macrophage influx, reperfusion hemorrhage) in much of the examined brain, particularly the supratentorial tissues, and the strong correlation with measures of perfusion utilized in the determination of brain death (such as radioisotope scintigraphy). According to Pearson et al (4), cases with a clinically detectable radioisotope bolus had reactive brain changes, while those without had “autolysis,” i.e. “tissue breakdown that is dependent on intrinsic cellular enzymes and independent of factors derived from flowing blood”. Any focal reactive changes thus are considered to reflect “neuronal necroses . . . [that] arise at different rates within the cerebral cortex and the lower brainstem,” further suggesting zones of incomplete or agonal cerebral ischemia (5).

In those published cases neuropathologically evaluated after longer intervals (months to years), neuropathologic changes were quite like the current case (Table 2). Parisi et al (9) described, after a 68-day interval, dural sinus thrombosis, “cortical subpial vascularization and macrophages” and “coagulative necrosis but . . . no evidence of cellular reactivity” of deeper structures. As in our case, this combination of findings suggested to the authors an “inward progression of the reparative response from the leptomeningeal surface, presumably originating from the intact extracranial circulation.” Similarly, “proliferation of vessels and fibrosis . . . [and] erythrocytes, leucocytes and scavenger cells in the dura mater” were described after 101 days by Ito (10). “Secondary petechial haemorrhage[s]” . . . “appear to occur long after the trauma, in spite of the complete cessation of cerebral blood flow” . . . [and] “may be produced from newly formed vessels in the dura mater by secondary circulatory disturbances” . . . [since] “the blood flow of the dura is maintained by the middle meningeal artery which originates from the external carotid artery” (10). A singular case reported by Repertinger et al (11) after an interval of 20 years was notable for an outer “calcified shell,” with ossification and, as in our case, hematopoietic marrow, encasing grumous mummified material, iron pigment, mineralized cell processes, and extensive small focal calcifications. These contrast somewhat with our findings of macroscopically distinct cerebral and cerebellar cortices, as well as faint cellular outlines of neurons and other structures. We speculate that the nature of the cause of brain death in their case (specifically, meningitis, in which inflammatory cells were already “on board” before brain death declaration), and the additional interval of 15 years may account for some of these differences. Regardless, their estimation of the pathophysiology that “blood flow was insufficient over the 2 decades for macrophages to arrive and remove most of the debris” largely concurs with ours (11).

### Final points

In closing, we share the unique and complex neuropathologic findings of Ms Jahi McMath, an extraordinary young woman.

While unable to correlate our analyses with the clinical and radiographic observations of years earlier, we are very grateful for this unprecedented opportunity to expand the spectrum of observed human brain tissue alterations in a very rarely encountered set of biologic conditions. We owe a promise to her, her family, and her caregivers to continue to learn as we refine our notions of brain death, of postischemic tissue reaction and the importance of careful autopsy examination.

### ACKNOWLEDGMENTS

We gratefully acknowledge Ms Nailah Winkfield and Mr Christopher Dolan for their trust in us as we did our best to analyze the autopsy photographs, reports, and brain tissue specimens of Ms Jahi McMath. Dr Gina Prochilo originally participated in the autopsy and kindly reviewed the manuscript for accuracy regarding some of the methods. Drs Sarah Thomas and Gregory Dickinson generously shared examples of the other postmortem changes illustrated here for comparative purposes. We are thankful to Mr Valeriy Bhukarov in the Neuropathology Brain Bank & Research CoRE at the Icahn School of Medicine for his histological support. Ms Jill Gregory, MFA, CMI, provided our medical illustration. Ms Tara Key and Ms Elisabeth Haas assisted in obtaining some of the historical references. Dr Hannah C. Kinney was helpful in her critical reading of the manuscript.

### CONFLICT OF INTEREST

The authors have no duality or conflicts of interest to declare.

### REFERENCES

- Greer DM, Shemie SD, Lewis A, et al. Determination of brain death/death by neurologic criteria: The world brain death project. *JAMA* 2020;324:1078–97
- Wijdicks EF, Varelas PN, Gronseth GS, et al.; American Academy of Neurology. Evidence-based guideline update: Determining brain death in adults: Report of the Quality Standards Subcommittee of the American Academy of Neurology. *Neurology* 2010;74:1911–8
- Seifi A, Lacci JV, Godoy DA. Incidence of brain death in the United States. *Clin Neurol Neurosurg* 2020;195:105885
- Grunnet ML, Paulson G. Pathological changes in irreversible brain death. *Dis Nerv Syst* 1971;32:690–4
- Walker AE, Diamond EL, Moseley J. The neuropathological findings in irreversible coma. A critique of the “respirator”. *J Neuropathol Exp Neurol* 1975;34:295–323
- Pearson J, Koren J, Harris JH, et al. Brain death: II. Neuropathological correlation with the radioisotopic bolus technique for evaluation of critical deficit of cerebral blood flow. *Ann Neurol* 1977;2:206–10
- Schroder R. Later changes in brain death. Signs of partial recirculation. *Acta Neuropathol* 1983;62:15–23
- Wijdicks EF, Pfeifer EA. Neuropathology of brain death in the modern transplant era. *Neurology* 2008;70:1234–7
- Parisi JE, Kim RC, Collins GH, et al. Brain death with prolonged somatic survival. *N Engl J Med* 1982;306:14–6
- Ito Y, Kimura H. Early and late meningeal reaction to trauma after long-term brain death. *Forensic Sci Int* 1992;56:189–94
- Repertinger S, Fitzgibbons WP, Omojola MF, et al. Long survival following bacterial meningitis-associated brain destruction. *J Child Neurol* 2006;21:591–5
- Aviv R. *What Does It Mean to Die?* New York, NY: Conde Nast; 2018.
- Shewmon DA, Salamon N. The extraordinary case of Jahi McMath. *Perspect Biol Med* 2021;64:457–78
- Shewmon DA, Salamon N. The MRI of Jahi McMath and its implications for the global ischemic penumbra hypothesis. *J Child Neurol* 2022;37:35–42
- Dekaban AS. Changes in brain weights during the span of human life: Relation of brain weights to body heights and body weights. *Ann Neurol* 1978;4:345–56
- Doran GH, Dickel DN, Ballinger WE Jr, et al. Anatomical, cellular and molecular analysis of 8,000-yr-old human brain tissue from the Windover archaeological site. *Nature* 1986;323:803–6
- Salihbegovic A, Clark J, Sarajlic N, et al. Histological observations on adipocere in human remains buried for 21 years at the Tomasica grave-site in Bosnia and Herzegovina. *Bosn J Basic Med Sci* 2018;18:234–9
- Ubelaker DH, Zarenko KM. Adipocere: What is known after over two centuries of research. *Forensic Sci Int* 2011;208:167–72
- Prats-Munoz G, Malgosa A, Armentano N, et al. A paleoneurohistological study of 3,000-year-old mummified brain tissue from the Mediterranean bronze age. *Pathobiology* 2012;79:239–46
- Kleinschmidt-DeMasters BK, Lillehei KO, Hankinson TC. Review of xanthomatous lesions of the sella. *Brain Pathol* 2017;27:377–95
- Pendleton C, Jiang B, Geocadin RG, Quinones-Hinojosa A. “Any possible restoration of function could not occur”: Harvey Cushing and the early description of brain death. *World Neurosurg* 2012;77:394–7
- Alderete JF, Jeri FR, Richardson EP Jr, et al. Irreversible coma: A clinical, electroencephalographic and neuropathological study. *Trans Am Neurol Assoc* 1968;93:16–20
- Adams RD, Jéquier M. The brain death syndrome: Hypoxemic pan-encephalopathy. *Schweiz Med Wochenschr* 1969;99:65–73
- Astrup J, Siesjo BK, Symon L. Thresholds in cerebral ischemia—The ischemic penumbra. *Stroke* 1981;12:723–5
- Harish G, Mahadevan A, Pruthi N, et al. Characterization of traumatic brain injury in human brains reveals distinct cellular and molecular changes in contusion and pericontusion. *J Neurochem* 2015;134:156–72
- Haseldonckx M, van Bedaf D, van de Ven M, et al. Vasogenic oedema and brain infarction in an experimental penumbra model. *Acta Neurochir Suppl* 2000;76:105–9
- Bernat JL. Refinements in the organism as a whole rationale for brain death. *Linacre Q* 2019;86:347–58
- Truog RD, Berlinger N, Zacharias RL, et al. Brain death at fifty: Exploring consensus, controversy, and contexts. *Hastings Cent Rep* 2018;48(Suppl 4):S2–5
- Young MJ, Bodien YG, Giacino JT, et al. The neuroethics of disorders of consciousness: A brief history of evolving ideas. *Brain* 2021;144:3291–310
- Scott RM, Smith ER. Moyamoya disease and Moyamoya syndrome. *N Engl J Med* 2009;360:1226–37
- Mukawa M, Nariai T, Inaji M, et al. First autopsy analysis of a neovascularized arterial network induced by indirect bypass surgery for Moyamoya disease: Case report. *J Neurosurg* 2016;124:1211–4
- Del Bigio M. Autolysis and artifacts. In: Lechpammer M, Del Bigio M, Folkerth R, eds. *Perinatal Neuropathology*. Cambridge, United Kingdom: Cambridge University Press; 2021:131–8
- Genest DR, Williams MA, Greene MF. Estimating the time of death in stillborn fetuses: I. Histologic evaluation of fetal organs; an autopsy study of 150 stillborns. *Obstet Gynecol* 1992;80:575–84
- Simcock IC, Shelmerdine SC, Langan D, et al. Micro-CT yields high image quality in human fetal post-mortem imaging despite maceration. *BMC Med Imaging* 2021;21:128

35. Hess MW, Klima G, Pfaller K, et al. Histological investigations on the Tyrolean Ice Man. *Am J Phys Anthropol* 1998;106: 521–32
36. Leccia C, Alunni V, Quatrehomme G. Modern (forensic) mummies: A study of twenty cases. *Forensic Sci Int* 2018; 288:330.e1–9
37. Shedge R, Krishan K, Warriar V, et al. *Postmortem Changes*. Treasure Island, FL: StatPearls; 2022.
38. Kumar V, Abbas A, Aster J, eds. *Cellular responses to stress and toxic insults: Adaptation, injury, and death*. Robbins and Cotran Pathologic Basis of Disease, 8th ed. Philadelphia: Saunders Elsevier; 2010:14–5